Molecular Crystals and Liquid Crystals

Publication details, including instructions for authors and subscription information:
http://www.tandfonline.com/loi/gmcl20

Photorefractive-Like All-Optical Switching in Nematic-Photoconducting Polymer Liquid Crystal Cell

Andrzej Miniewicz [a], Jaroslaw Mysliwiec [a], Piotr Pawlaczyk [a] & Marcin Zielinski [a]

[a] Institute of Physical and Theoretical Chemistry, Wroclaw University of Technology, Wybrzeze Wyspianskiego, Wroclaw, Poland

Version of record first published: 05 Apr 2011

To cite this article: Andrzej Miniewicz, Jaroslaw Mysliwiec, Piotr Pawlaczyk & Marcin Zielinski (2008): Photorefractive-Like All-Optical Switching in Nematic-Photoconducting Polymer Liquid Crystal Cell, Molecular Crystals and Liquid Crystals, 489:1, 119/[445]-134/[460]

To link to this article: http://dx.doi.org/10.1080/15421400802219718

Mol. Cryst. Liq. Cryst., Vol. 489, pp. 119/[445]–134/[460], 2008

ISSN: 1542-1406 print/1563-5287 online
DOI: 10.1080/15421400802219718

Taylor & Francis
Taylor & Francis Group

Photorefractive-Like All-Optical Switching in Nematic-Photoconducting Polymer Liquid Crystal Cell

Andrzej Miniewicz, Jaroslaw Mysliwiec, Piotr Pawlaczyk, and Marcin Zielinski
Institute of Physical and Theoretical Chemistry, Wroclaw University of Technology, Wybrzeze Wyspianskiego, Wroclaw, Poland

Nematic liquid crystals are highly optically nonlinear materials. Third order optical nonlinearities can be viewed through light intensity dependent refractive index. We exploit this nonlinearity in a specially designed planar liquid crystalline panel composed of highly birefringent nematic and photoconducting polymer to construct optically addressed spatial light modulator. The system described in this work shows photorefractive-like behavior enabling holographic animations in real-time. We also present all-optical switching using one laser source to create the grating and another one to modify the external electric field applied to the panel and resulting in switching of diffracted light intensity of the former.

Keywords: dynamic holography; liquid crystal; optical switching; spatial light modulator

1. INTRODUCTION

Nonlinear optics offers a variety of phenomena allowing for laser light manipulation through the third order effects. Self-phase modulation effects can be described by the well known relation of nonlinear refractive index: $n(I) = n_o + n_2 I$, where n_o is a low-intensity refractive index, I is the light intensity and n_2 nonlinear coefficient charactersitic for material and dependent on frequency and mechanism of light-matter interaction. In most materials this coefficient is extremely low but in liquid crystals (LC's) it becomes gigantic reaching values of $n_2 \cong 10^{-3}\,\mathrm{cm}^2/\mathrm{W}$ [1,2]. From the above formula it follows that using

We acknowledge financial support of Polish Ministry of Science and Higher Education within project No. N507 132 31/3302 and Wroclaw University of Technology.

Address Correspondence to A. Miniewicz, Institue of Theoretical and Physical Chemistry, 50-370 Wroclaw, Poland. E-mail: andrzej.miniewicz@pwr.wroc.pl

a moderate laser light intensity, of the order of 10^2 W/cm^2, refractive index can be changed on a level of 0.1. This is sufficient to effectively change the direction of light beam, its phase or frequency. Moreover, such a huge nonlinearity opens a possibility to use spatially modulated light to spatially change the refractive index of the liquid crystal. However, there are some drawbacks. The nematic liquid crystal must be in one of its aligned textures: homeotropic or planar otherwise the large amount of incoming light is scattered on micro-size domains. The alignment of LC induced by surface treatment requires that the thickness of the liquid crystal layer is limited to a small fraction of 1 mm, usually below 50 μm. Short light path through a nonlinear medium limits the total performance of a photonic device. The unique feature of a strong optical nonlinearity present in a specially prepared LC panels allowed to use spatially modulated in intensity light $I(x,y)$ to address the device. Classic Spatial Light Modulator (SLM) is a real-time device able to spatially modulate amplitude, polarization and/or or wave front of a light wave that is transmitted through or reflected by it. The SLMs allow for a control of the corresponding spatial positions independently. The majority of contemporary SLMs have emerged from devices that were originally intended either for image storage or projection display, both with incoherent light readout as well as coherent one [3]. Most of them have pixelated structure with electrical addressing (EA) of each pixel. The constant development of SLM technology has opened up many new applications especially because an SLM can be addressed by simply connecting it to a computer as an external monitor. SLMs will soon be widely used components, not only for conventional video projection applications based on amplitude modulation, but also in applications based on phase or polarization modulation. The most spectacular use of SLM is in holographic optical tweezers [4], adaptive optics [5], holographic optical storage [6] and even in holographic image projection for head-up displays. Dynamically addressable, SLMs can be thought of a switchable alternative to classic optical components, such as projection slides, apertures, lenses, diffraction gratings, beam splitters and retardation waveplates. Presently, there are two common SLM implementations: a micromechanical SLM that uses arrays of movable micromirrors and an electro-optical SLM that uses various types of liquid crystal-based microdisplays.

We focus our attention to nematic LC-based optically driven devices that can be translucent and reflective and working at switching frequencies of several tens Hz. Envisaged is also the cell based on ferroelectric LC's having just two different molecular orientations [7]. This restricts the cell switching properties to binary modulation of the light

field but the accessible switching time is very short and signals can be displayed at kHz frequencies.

Nematic LC materials with the planar and twisted nematic (TN) configurations are the mostly exploited ones. Application of an electric field E to the transparent electrodes of the LC cell, makes that molecules take a field dependent position $\theta(E)$ and tend to align toward the electric field lines. When crossed polarizers are used the modulator acts as an amplitude modulator, even for white light sources. The intermediate greyscale transmission is available with the typical switching times ranging from 5–20 ms. Planarly aligned nematic (PAN) cells comprise two parallel director plates. The molecules' axes are parallel for all voltage levels and the cell acts as an optical retardation plate with a variable retardation. This makes PAN cells ideal for use as amplitude modulators, phase modulators and polarization rotators. Important parameter is the number of pixels and their size. Nowadays SLMs with up to 1920×1200 pixels are available.

The presence of a fixed pixellated structure is not advantageous for some of the applications due to unavoidable laser light diffraction and absorption. Therefore there is an effort devoted to develop, similar in principle, SLM devices that could be steered directly by light a so called optically addressed SLMs (OA SLM's). For certain type of applications the optical addressing is the only solution [8–11]. Optically addressed liquid crystalline spatial light modulator (OA LC SLM) in which optical transmittance properties are controlled by another optical beam, plays a key role in many optical information—processing systems. The mechanism of spatial control over local refractive index of LC cell, exploited in this work, is related to the surface electric potential changes due to photoconductivity of polymeric layer serving also as an alignment layer. Low operating voltages, high diffraction efficiency on grating structures, reversibility of the process and acceptable times of response to the light pulses make this OA LC SLM attractive for the dynamic holography applications. Various implementations of the OA LC SLM like: optical phase conjugation, optical correlation, incoherent-to-coherent image conversion and wave-front correction have been described in several previous papers by our group [12–17].

In this work we describe the unconventional use of OA LC SLM for optical switching and dynamic hologram retrieval using visible as well as an infrared laser light source.

2. EXPERIMENTAL

We assembled the PAN liquid crystal panel composed of a thin layer of photoconducting polymer on one side and a conventional polyimide on

another side and filled it with highly birefringent nematic liquid crystalline (LC) mixture. The used 14 component LC mixture (purchased from MUT, Warsaw, Poland) is characterized by the refractive indices at 589 nm $n_o = 1.5307$, $n_e = 1.8728$, birefringence $\Delta n = 0.3421$, rotational viscosity $\gamma = 104$ mPa s and a clearing temperature $T_I = 155^oC$. Optical stability of the mixture ensures the long operational time of the device.

The structure of the optically addressed liquid crystal spatial light modulator is asymmetrical and composed of two ITO-covered glass plates with inner parts covered by spin-coated thin layers ($\sim$100–200 nm) of a photoconducting polymer on one side and of polyimide orienting layer on the another (cf. Fig. 1a). The deposited polymeric thin films exhibited good optical quality and homogeneity over the whole display area (10 cm $\times$ 5 cm). Both layers before assembling of a cell were uniaxially rubbed. Thickness of the LC layer was 10 μm. As the photoconducting polymer we have used a poly(N-vinyl carbazole) (PVK) form Aldrich (Fig. 1b). In order to ensure better planar alignment the cell was composed in an antiparallel fashion, though nothing is known about anchoring properties and the pretilt angle on PVK due to application of standard rubbing procedure. In order to induce photoconductivity in the visible part of the spectrum we doped PVK

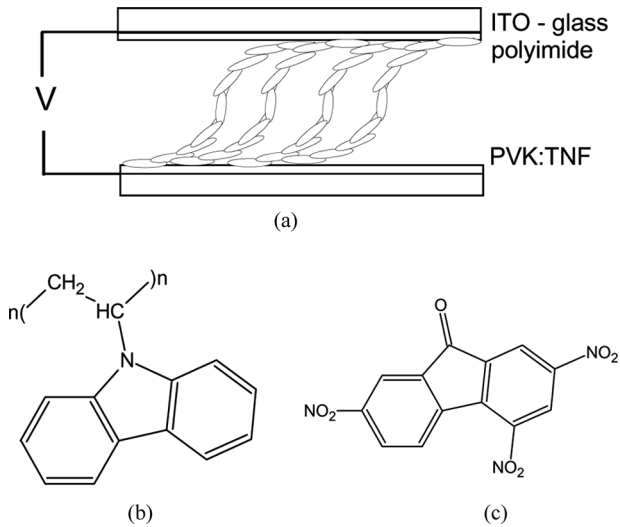

FIGURE 1 Schemeof LC panel (a) and chemical structures of (b) poly(N-vinyl carbazole) and (c) 2,4,7-trinitrofluorenone – forming the photoconducting polymer.

with 2,4,7-trinitrofluorenone (TNF) (Fig. 1c) at the 10:1 wt/wt ratio enabling charge transfer complex formation between PVK units and TNF. Absorption coefficient α of 8–14 cm^{-1} was measured within the charge transfer CT absorption band. Such a doping results in the effective hole mobility of the order of 10^{-6} cm^2/Vsand electron mobility of the order 10^{-9} cm^2/Vs in this polymer [18]. This difference in charge carrier mobilities is crucial for the efficient light-induced surface electric potential changes.

Light of 514.5 nm and 632.8 nm wavelength from Ar^+ and He-Ne lasers is suitable for the photogeneration of charge carriers in the photoconducting polymer layer under dc electric field applied to LC cell. The speed of the internal space-charge field buildup in the PVK:TNF layer depends on charge generation, transport and trapping. Charge generation and transport determine photoconductivity σ_{ph} , which is defined as:

$$\sigma_{ph} = ne\mu = \frac{\phi\alpha \cdot I\tau}{h\nu} e\mu \tag{1}$$

where n is the density of free charge carriers, e is the elementary charge, μ is the mobility, Φ is the charge generation quantum efficiency, α is the absorption coefficient, I is the light intensity, τ is the time constant for transport, h is Planck's constant, and ν is the frequency of the light. The speed of space-charge field formation in polymer PVK:TNF is therefore proportional to the light intensity I.

Depending on ITO electrode polarization more mobile photogenerated holes are removed from the polymer layer or are pushed away toward the opposite electrode via ionic transport through LC layer. Less mobile electrons stay longer within polymer layer thus forming a spatially modulated potential on the surface. The detailed process of electric field formation and decay in such a system is relatively complex. Many research group contributed to the knowledge about the possible processes influencing the orientation of LC molecules in similar systems pointing on photoconductivity induced anchoring changes at the surface, hole and electron redistribution in photoconducting polymer, charge double layer formation at the interface and ion transport through LC layer [19–25].

3. DYNAMIC HOLOGRAPHY IN IR RANGE

Dynamic (interrupted) illumination of OA LC SLM causes temporary surface charge build-up and decay. Supposing that nonuniform spatially light $I(x,y)$ is incident on the LC panel the replica of refractive index spatial modulation $n(x,y) = n_0 + n_2 I(x,y)$ is formed. So the

formation of phase-only gratings or holograms in LC panel is possible. We tested the dynamic properties of the OA LC SLM's attempting to optically reconstruct the holograms temporally projected onto the LC panel. For that purpose we used the computer controlled multimedia projector (cf. experimental set-up shown in Fig. 2) for display simple binary holograms (computer generated holograms – CGH) and extraordinary polarized laser light beam for hologram retrieval.

These holograms, demagnified with the help of a suitable optics, were displayed directly at the surface of the PVK:TNF layer of the LC panel. In order to facilitate the adequate focusing the optically addressed liquid crystal spatial light modulator was placed on a micrometer precision moving stage. Holograms of size $1 \times 1\,\mathrm{cm}^2$ were reconstructed with a collimated laser beam expanded to a diameter of about 1 cm in order to illuminate the whole area of the phase hologram. The fidelity of the optically reconstructed image with respect to the calculated one is shown in Figure 3. We used this system for the demonstration of a real-time optical binary hologram reconstruction in the visible part of the spectrum ($\lambda = 632.8\,\mathrm{nm}$) but also in the infrared ($\lambda = 904\,\mathrm{nm}$) using a laser diode.

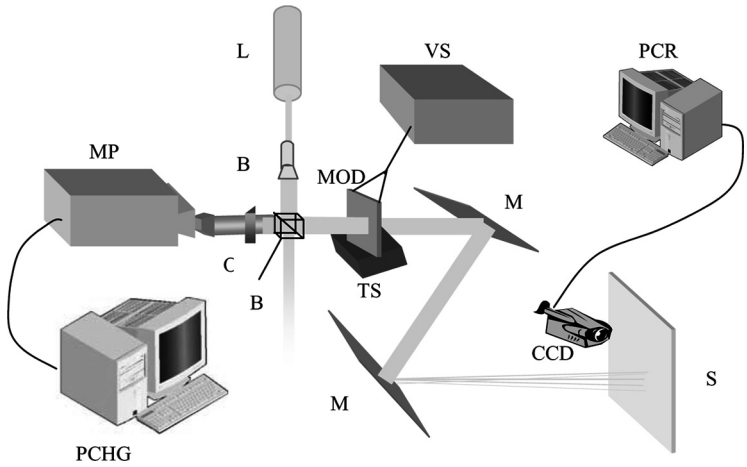

FIGURE 2 Schematic representation of the optical set-up for static and dynamic retrieval of binary holograms projected on OA LC SLM; L – reading laser He-Ne 632.8 nm or laser diode 904 nm, BE – beam expander, O – objective f = 135 mm, BS – beam splitter, MOD – OA LC SLM, TS – precise translation stage, VS – voltage supplier, M – mirror, S – screen, CCD-camera, PCR – computer registering reconstructed holograms, PCGH computer used for sending holograms of 2-D objects to multimedia projector MP.

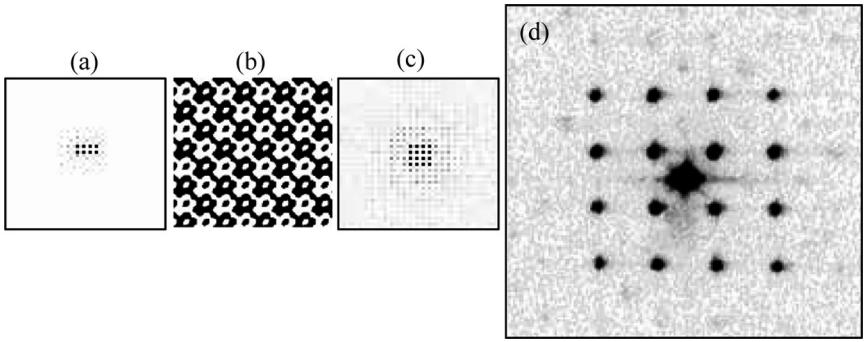

FIGURE 3 An example of a target (a) its binary hologram (b) numerically reconstructed image (c) and optically reconstructed one (d). The hologram was projected on OA LC SLM via multimedia projector. The symmetry of binary hologram results in appearance of conjugate image for numerical (c) and optical reconstruction (d).

The binary holograms were prepared numerically with the help of Holomaster 2.0 code from the predesigned targets and using a direct binary search method [16]. The size of the reconstructed object observed at the screen depended on the total size of a hologram projected onto OA LC SLM and a distance between OALC SLM and the screen. The object size can be enlarged by decreasing the size of the projected hologram with a lens system. The limit of the object size and spatial resolution of its features are related with a spatial resolution of the LC and projection systems. Separate pixels as defined in the target (cf. Fig. 3) are well seen in the far field of reconstructed hologram. Spatial resolution of our LC panel, as calculated from a virtual pixel size, is better than 50 lines per millimeter. The maximum resolution estimated from the separate grating recording experiments using two-wave mixing technique and laser light reaches 250 lp/mm. For the first time, what is presented in this work, we achieved an optical hologram reconstruction using IR laser source ($\lambda = 904\,\text{nm}$) in transmissive OALC SLM. The diffraction efficiency at 904 nm was smaller than for 633 nm light due to decrease in liquid crystal birefringence at IR spectral range with respect to the visible part of the spectrum. The holographic properties of the LC panel have been measured in function of incoming light intensity, color of light used to project holograms, spatial resolution and dynamics of holographic illumination in order to optimize the recording conditions.

OA LC SLM could be operated within the range of 2–30 V, however for the best performance OA LC SLM requires the dc voltage set

within a relatively small range. For a given input light intensity the voltage applied to the panel has to be tuned in order to get the best contrast at the far field image. Response and recovery times to the changing light scenario depend on many factors and for nematics are typically: time-on ≈10–30 ms and time-off ≈50–200 ms. These limits originate from the photoconductive properties of PVK:TNF polymer and ion mobilities in LC and the thicknesses of the respective layers. For study of these factors we prepared the series of gratings in the form of equally separated fringes black and white or color-black. Then we projected them onto panel in a specially designed time varying sequences, i.e. grating followed by a black screen. Due to an appearance of the grating on a LC panel the light was diffracted and we set a photodetector at the first order diffraction direction measuring the response with the help of an oscilloscope. In Figure 4 the rise-time of the grating build-up is plotted versus voltage applied to the LC panel. One can notice that the maximum response time occurs at about −6 V or +7 V and amounts to 200 ms, whereas for higher voltages it drops to about 50 ms.

The observed maxima are connected with the easiest molecular orientation that occurs when most of the LC molecules are directed at an angle of 45° with respect to the cell surface.

Next we checked the diffraction signal dependence on color of the displayed grating. Initially we used the "black and white" gratings (dark-white pixels), however for the experiment presented in

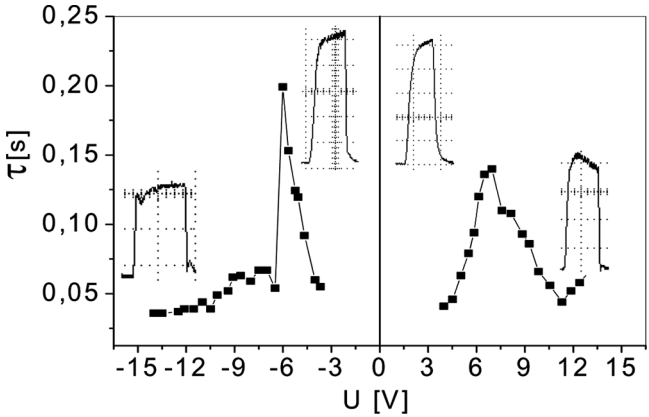

FIGURE 4 Rise time of the grating build-up as observed by measurement of first order diffraction signal on phase grating formed in OA LC SLM in function of dc voltage applied to the panel. Insets show the exemplary shapes of signals observed when grating is switched-on and-off.

Figure 5 the gratings were of black and color type (dark-color pixels). The result was unexpected, as we noticed, that the highest diffraction efficiency was obtained for the "green-black" grating while the lowest one for the "blue-black" grating. The "white-black" grating showed the efficiency close to "red-black" grating. In order to understand this result we have measured the spectra of light coming form the projector for different color gratings which are shown in Figure 6. Obviously the dependence of light diffraction on color of the grating is due to efficiency of charge carrier production in PVK-TNF polymer and the light flux send from the projector for a given displayed color. The conclusion from this part of the study is that the projection of a "white-black" grating is less efficient than the "green-black" one.

In Figure 7 we present the diffraction pattern obtained for the gratings projected in visible light onto LC panel but read with infrared laser light beam of $\lambda = 904\,\text{nm}$. The photographs were taken by a CCD camera with Si-detectors which are quite sensitive in this spectral range.

We realized the video holographic animations (cf. Fig. 7b) in infrared spectral range. The switching time between the holograms was 50 ms. The maximum of diffraction efficiency was observed for dc voltage equal 15 V and amounted to $\eta = P_1/P_0 \cong 0.3\%$ for a studied panel for IR reading beam (cf. Fig. 8). Comparison of diffraction efficiency $\eta_1 \approx (\Delta\phi)^2/4$ for the same grating for visible and IR light contains the information about the birefringence at the respective light

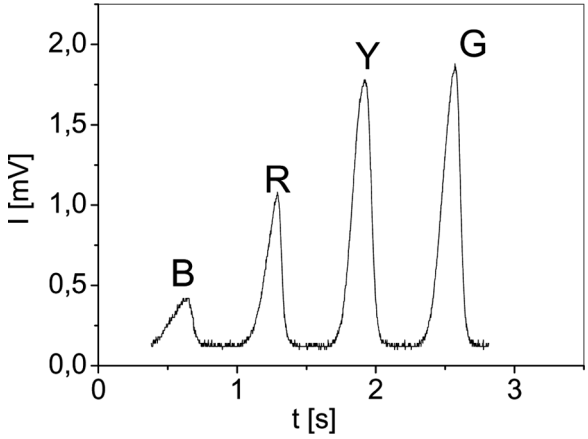

FIGURE 5 Observation of a first order diffraction signal magnitude for a sequence of four different color gratings projected onto OA LC SLM. B – blue-black, R – red-black, Y – yellow-black and G – green-black.

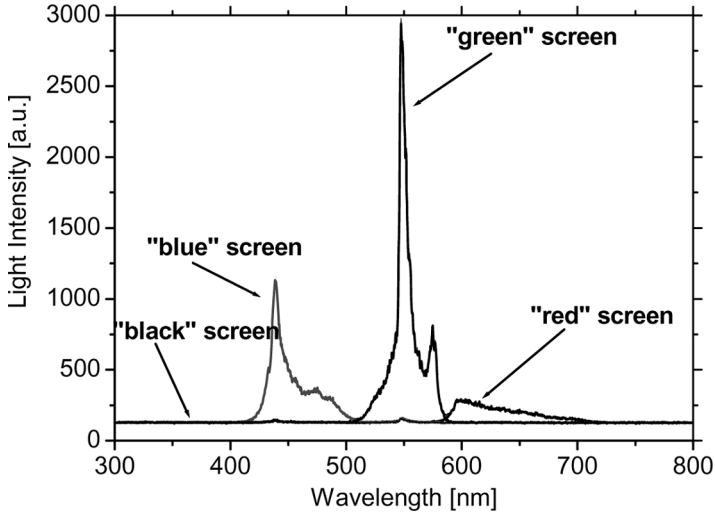

FIGURE 6 Spectra of light emitted form projector when the color of screen is set to black, red, blue, green and white. The white screen is composed of blue, green and red light having the same intensities as that shown in the figure.

wavelengths as the phase delay due to grating is $\Delta\phi = 2\pi\Delta nd/\lambda$, where Δn is the amplitude of spatial modulation of refractive index in LC layer. From the experiment we have found that effective grating amplitude induced by light amounts to $\Delta n = 1.57 \times 10^{-3}$ at 904 nm what is equivalent to 0.5% use of the accessible LC birefringence.

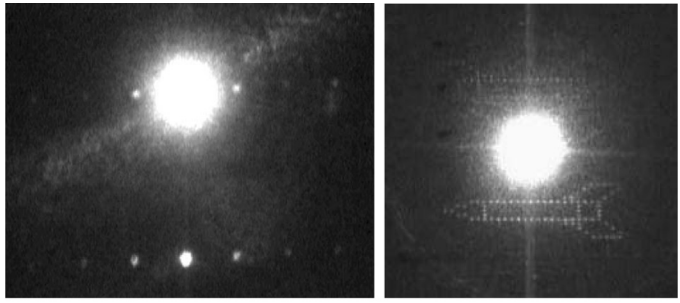

FIGURE 7 The photograph of diffraction spots of 904 nm laser beam scattered on a phase grating formed in LC panel by visible light (a) and the single frame of image from holographic animation in IR (b). The image is taken by a CCD camera as it is invisible for a naked eye.

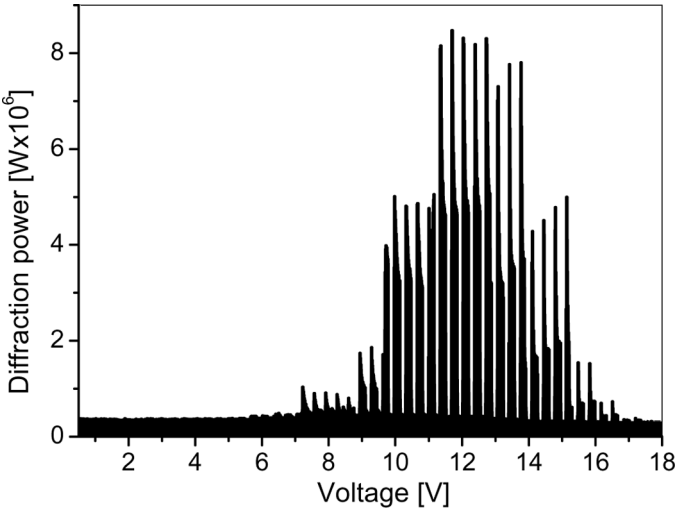

FIGURE 8 Dependence of power of 904 nm light diffracted into first order on the grating with 70.4 μm period created in the studied OA LC SLM. Incident light power $P_o = 2.8 \times 10^{-4}$ W.

4. ALL-OPTICAL SWITCHING

Besides the holographic applications we used the same LC panel to observe all-optical switching in a novel geometry. All-optical switching was realized with the anti-parallel converging two-beam coherent laser light illumination using continuous wave laser emitting light at 632.8 nm and Nd:YAG cw laser working at 532 nm wavelength for the steering. Scheme of the experimental set-up realizing all-optical switching is shown in Figures 9 and 10, where the details of red light scattering due to bulk phase grating with wavevector **K** and the influence of the external green laser light on this scattering due to the modification of surface potential are shown.

The idea was to exploit the huge optical nonlinearity of the nematic liquid crystal and create a co-linear circular type holographic grating in the bulk of the LC layer like in the experiment that has been presented [26] for rubidium vapors. In the described in Ref. 26 experiment for the low-power illumination an instability of scattered light had occurred, that was switched in position with an extremely low external light directed off-axis. In this way an optical transistor has been demonstrated [26]. We repeated the geometry of the above mentioned experiment forming the grating inside the LC volume with the period of ca. $\Lambda = 0.2\,\mu m$ ($\Lambda = \lambda/2n$). In order to induce light scattering the

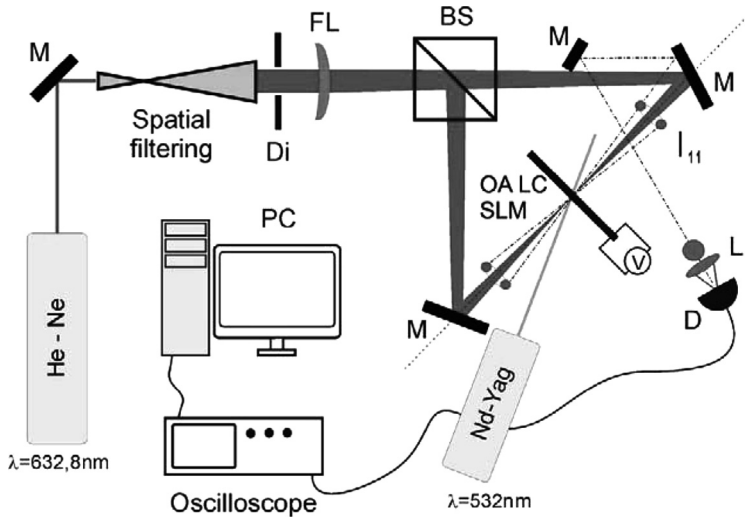

FIGURE 9 Experimental set-up for studying of all-optical switching in OA LC SLM in counter-propagating beam geometry. The interference of two 632.8 nm beams forms a grating in the LC panel and the grating strength is disturbed by an external light coming from doubled in frequency Nd-YAG laser (532 nm). FL – Fourier lens, Di – diaphragm, D – detector, M – mirror.

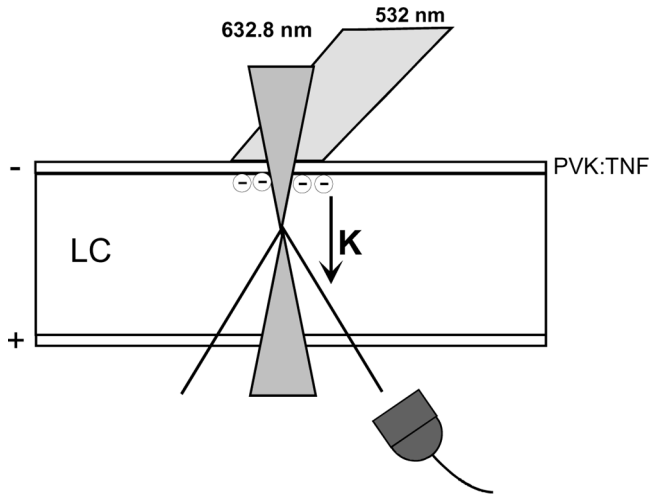

FIGURE 10 Schematic view of light scattering into first order diffraction order on grating made in LC panel by two converging and counter propagating laser beams and role of external light in changing electric field acting on LC molecules forming the grating.

application of dc external field is necessary to overcome the Freedericksz threshold and move molecules from their homogenic alignment toward partially homeotropic one. The grating results due to optical torque which the incident spatially modulated in intensity red light imposes on the liquid crystal molecules, i.e. like in an orientational optical Kerr effect. Due to beam convergence the strongest optical Kerr effect arises at or close to their focal point. Therefore both beams should be focused exactly at the cell center. Around the focal point light intensity is large and molecules are more susceptible to reorientation because their long axes are inclined from the direction of electric field of the red beam. Moreover the molecules placed in the cell center can be tilted easier from their equilibrium positions than the molecules positioned in the proximity of the surfaces due to anchoring. Light scattered into first order diffraction on such a grating should form rings outside the incoming zero-order beams. However, in present study we could see only two spots of first order diffraction placed in the plane orthogonal to the rubbing direction. This is result of circular light pattern symmetry breaking already by the cell preparation method i.e. planar alignment at the surfaces. For light polarized perpendicular to the n_e axis the sufficiently large refractive index grating can arise. The green light from the doubled in frequency YAG laser incident on the area where the gratings are formed serves simply as a source of photogeneration of charge carriers in the PVK:TNF layer. Externally applied electric field helps to separate charge carriers and their flow decreases the effective electric field strength acting on LC molecules in the bulk of the LC layer under illuminated spot. Decrease of electric field acting on LC molecules change their position and according to that also the effectiveness of their reorientation by optical field.

In reported experiment the addressing light intensity amounted to $I_{\mathrm{ADR}} = 1{,}79\,\mathrm{mW/cm^2}$ ($\lambda = 632.8\,\mathrm{nm}$) and the control beam from Nd-YAG ($\lambda = 532\,\mathrm{nm}$) had slightly lower intensity $I_{\mathrm{C}} = 0.40\,\mathrm{mW/cm^2}$. Depending on the voltage applied to the OA LC SLM we could observe green light induced changes in intensity of the scattered into first diffraction order red light. These changes were either positive or negative depending on magnitude of dc voltage applied to the panel, what is illustrated in Figure 11. Thus we demonstrate the possibility of steering the red light intensity by a green light. An analysis of the phenomenon showed that the changes of diffraction signal power $\delta \mathrm{P}_1(\mathrm{U})$ can be an indication of the second derivative of an effective refractive index $n_e^{eff}(U)$ of LC mixture over the voltage as seen by 632.8 nm light, providing the disturbing light intensity of 532 nm beam is weak. The effective voltage applied to the panel depends on light illumination

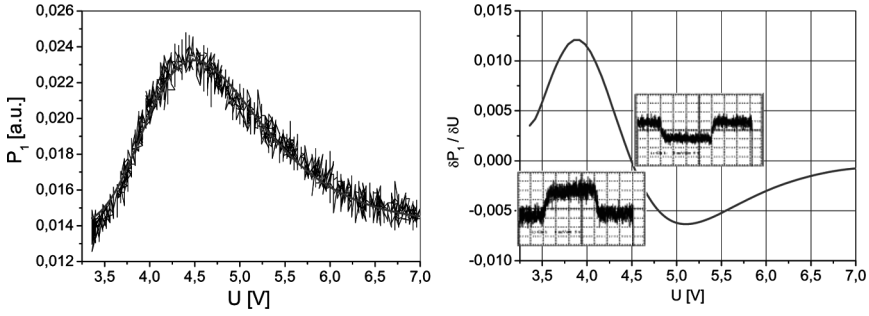

FIGURE 11 Power of 632.8 nm light diffracted on a grating formed by collinear anti-parallel beams in OALC SLM in function of voltage (a) and changes in diffraction induced by a weak 532 nm laser light (b) The observed on oscilloscope signals directly measure the second derivative of effective refractive index of the LC panel over dc voltage.

intensity: $U(I_{532}) = U_0 + \Theta \cdot I_{532}$, where coefficient Θ [Vcm^2/mW] describes the surface potential changes due to light illumination.

Experimentally observed diffraction efficiency changes $\Delta\eta(I_{532}) \propto \frac{\pi^2 \Delta n^2 (U(I_{532})) \cdot d^2}{\lambda^2}$ are dependent on light intensity I_{532} via square of diffraction grating amplitude created by red light. The use of the measured here characteristics in designing OA LC SLM for adaptive optics purposes is evident.

Thus we demonstrated a new original all-optical LC switch. Despite the fact that the positional switching (cf. Ref. [26]) has not yet been obtained for the LC panel the potential for such a switching still exists.

5. CONCLUSIONS

We have demonstrated the niche application of optically addressed liquid crystal spatial light modulators. The constructed by us device an OA LC SLM is suitable for mapping in a real time of phase holograms that could be retrieved either by coherent light from visible spectral range but also by infrared laser light. We also propose a new all-optical switch exploiting nonlinear optical Kerr effect in LC panel with photoconducting layer. Modulated external light was able to increase and/or decrease diffracted light intensity depending on the voltage applied to the LC panel. This phenomenon can serve as a tool for study OA LC SLM sensitivity to external light.

REFERENCES

[1] Khoo, I. C. (1995). *Liquid Crystals Physical Properties and Nonlinear Optical Phenomena*, J. Wiley: New York.

[2] Simoni, F. (1997). *Nonlinear Optical Properties of Liquid Crystals*, World Scientific Co.: Singapore.

[3] Ito, T., Shimobaba, T., Godo, H., & Hoiruchi, M. (2002). Holographic reconstruction with a 10 μm pixel-pitch reflective liquid-crystal display by use of a light-emitting diode reference light. *Optt. Lett. 27*, 1406–1409.

[4] Dufresne, E. R., Spalding, G. C., Dearing, M. T., Sheets, S. A., & Grier, D. G. (2001). Optical tweezer arrays and optical substrates created with diffractive optical elements. *Rev. Sci. Instr.*, *72*, 1810–1816.

[5] Gourlay, J., Love, G. D., Birch, P. M., Sharples, R. M., & Purvis, A. (1997). A real-time closed-loop liquid crystal adaptive optics system: First results. *Opt. Commun.*, *137*, 17–21.

[6] John, R., Joseph, J., & Singh, K. (2005). An input-data page modulation scheme for content addressable holographicdigital data storage. *Opt. Commun.*, *249*, 387–395.

[7] Talarico, M., Barbeiro, G., Pucci, D., Ghedini, M., & Golemme, A. (2003). Undoped photorefractive ferroelectric liquid crystal. *Adv. Mater.*, *15*, 1374–1377.

[8] Li, G., Erlap, M., Thomas, J., Tay, S., Schulzgen, A., Norwood, R. A., & Peyghambarian. N. (2005). All-optical dynamic correction of distorted communication signals using a photorefractive polymeric hologram. *Appl. Phys. Lett.*, *86*, 119–134.

[9] Feurer, T., Vaughan, J. C., Koehl, R. M., & Nelson, K. A. (2002). Multidimensional control of femtosecond pulses by use of a programmable liquid-crystal matrix. *Opt. Lett.*, *27*, 652–655.

[10] Efron, U., Wu, S. T., Grinberg, J., & Hess, L. D. (1985). Visible-to-Infrared dynamic image converter. *Opt. Eng.*, *24*, 111–116.

[11] Wu, S. T., Efron, U., & Hsu, T. Y., (1988). Near-IR-to-visible image conversion using a silicon liquid crystal light valve. *Opt. Lett.*, *13*, 13–15.

[12] Bartkiewicz, S., Sikorski, P., & Miniewicz, A. (1998). Optical image correlator realized with a hybrid liquid-crystal – photoconducting polymer structure. *Opt. Lett.*, *23*, 1769–1773.

[13] Bartkiewicz, S., Matczyszyn, K., Miniewicz, A., & Kajzar, F. (2001). High gain of light in photoconducting polymer – nematic liquid crystal hybrid structures. *Opt. Commun.*, *187*, 257–261.

[14] Miniewicz, A., Komorowska, K., Vanhanen, J., & Parka, J. (2001). Surface-assisted optical storage in nematic liquid crystal via photoinduced charge-density modulation. *Org. Electronics*, *2*(3–4), 155–163.

[15] Komorowska, K., Miniewicz, A., Parka, J., & Kajzar, F. (2002). Self-induced nonlinear Zernike filter realized with optically addressed liquid crystal spatial light modulator, *J. Appl. Phys.*, *92*(10), 5635–5641.

[16] Miniewicz, A., Gniewek, A., & Parka, J. (2002). Liquid crystals for photonic applications. *Opt. Mater.*, *21*, 605–610.

[17] Miniewicz, A., Mysliwiec, J., Kajzar, F., & Parka, J. (2006). On the real-time reconstruction of digital holograms displayed on photosensitive liquid crystal systems. *Opt. Mat.*, *28*(12), 1389–1397.

[18] Gill, W. D. (1972). Drift Mobilities in Amorphous Charge-Transfer Complexes of Trinitrofluorenone and Poly-n-vinylcarbazole. *J. Appl. Phys.*, *43*, 5033–5038.

[19] Merlin, J., Chao, E., Winkler, M., Singer, K. D., Korneychuk, P., & Reznikov, Y., (2005). All-optical switching in a nematic liquid crystal twist cell. *Opt. Express*, *13*, 5024–5030.
[20] Bartkiewicz, S., Miniewicz, A., Sahraoui, B., & Kajzar, F. (2002). Dynamic charge-carier-mobility-mediated holography in thin layers of photoconducting polymers. *Appl. Phys. Lett.*, *81*, 3705–3708.
[21] Kaczmaerk, M., Dyadusha, A., Slussarenko, S., & Khoo, I. C. (2004). The role of surface charge field in two-beam coupling in liquid crystal cells with photoconducting polymer layers. *J. Appl. Phys.*, *96*, 2616–2623.
[22] Barbero, G., Evangelista, L. R., & Madhusudana, N. V. (1998). Effect of surface electric field on the anchoring of nematic liquid crystals. *Eur. Phys. J. B 1*, 327–331.
[23] Tabiryan, N. V. & Umeton, C. (1998). Surface-activated photorefractivity and electro-optic phenomena in liquid crystals, *J. Opt. Soc. Am. B 15*, 1912–1917.
[24] Pagliusi, P. & Cipparone, G. (2002). Surface-induced photorefractive-like effect in pure liquid crystals. *Appl. Phys. Lett.*, *80*, 168–170.
[25] Zhang, J., Ostroverkhov, V., Singer, K. D., Reshetnyak, V., & Reznikov, Yu. (2000). Electrically controlled surface diffraction gratings in nematic liquid crystals. *Opt. Lett.*, *25*, 414–416.
[26] Dawes, A. M. C., Illing, L., Clark, S. M., & Gauthier, D. J. (2005). All-optical switching in rubidium vapor. *Science*, *308*, 672–674.